optica

Observation of the rotational Doppler shift of a white-light, orbital-angular-momentum-carrying beam backscattered from a rotating body

MARTIN P. J. LAVERY,* STEPHEN M. BARNETT, FIONA C. SPEIRITS, AND MILES J. PADGETT

School of Physics and Astronomy, University of Glasgow, Glasgow, UK

**Corresponding author: martin.lavery@glasgow.ac.uk*

Received 29 April 2014; accepted 29 May 2014 (Doc. ID 210521); published 22 July 2014

We observe the rotational Doppler shift of an orbital angular momentum (OAM)-carrying white-light beam after it is backscattered from a rotating object. Unlike the well known linear shift, this rotational shift is independent of the optical frequency, and hence each spectral component of the scattered light is shifted by the same value. Consequently, even a white-light source can give rise to a single-valued frequency shift. We show that the size of this shift is proportional to the OAM of the light and that superpositions of different OAM states give rise to multiple frequency sidebands. The observability of this rotational shift for white-light illumination highlights the potential for the rotational Doppler effect to form the basis of a rotational sensor for the remote detection of spinning objects.

OCIS codes: (000.2190) Experimental physics; (280.3340) Laser Doppler velocimetry; (280.7250) Velocimetry; (260.6042) Singular optics; (280.4788) Optical sensing and sensors; (280.1350) Backscattering.
http://dx.doi.org/10.1364/OPTICA.1.000001

The linear Doppler effect is the well-known frequency shift of a light beam that arises as a result of the relative motion between a source and an observer. This frequency shift scales with both the unshifted frequency and the linear velocity, an effect extensively used in Doppler velocimetry to detect the translational motion of surfaces and fluids [1,2]. Less well known than this linear effect is the rotational equivalent, where the frequency shift is proportional to the product of the rotational velocity between the source and the observer and the orbital angular momentum (OAM) of the light [3–8], such that $\Delta\omega = \ell\Omega$. Here, Ω is the angular rotational frequency and the illuminating field has an OAM of $\ell\hbar$ per photon. We reported recently that this rotational Doppler effect is manifest in monochromatic laser light backscattered from a spinning object, even in cases where the linear velocity between the source and observer is zero [9]. The effect has also been observed for a single point scatterer rotating about the optical axis of an illuminating beam [10]. In this last guise, the effect is similar to that predicted for the frequency shifts of atomic transitions when moving atoms are interrogated with light beams containing OAM [11]. The dependence of the rotational Doppler shift upon the angular momentum carried by the light means that in order to observe a single-valued shift, one needs to be selective in the angular momentum modes used either for illumination of the surface or in the detection of light scattered from it.

One striking feature of the rotational effect is that while the linear shift scales with the unshifted frequency, the rotational effect does not. Hence, for the rotational effect, all the frequencies within the same spatial mode of a white-light beam should be frequency shifted by the same amount. This ability to use white light suggests that the natural emission of light from a spinning object may result in a sufficiently large signal to allow the remote detection of spinning objects without the need for dedicated illumination.

In this present work we observe the rotational Doppler shift from a white-light source after it is backscattered by a spinning object. We show that the magnitude of this shift is dependent upon the OAM of the light, and that superpositions of different OAM states give rise to multiple sidebands on the shifted frequency. The observability of the frequency shift for white-light illumination highlights the potential of this rotational Doppler effect as the basis of a rotational sensor using backscattered light.

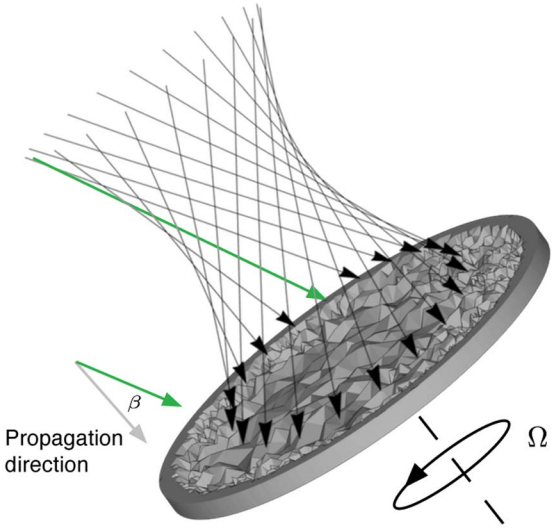

Fig. 1. For a helically phased beam (i.e., one carrying orbital angular momentum), the local ray direction is inclined by an angle $\beta = \ell/k_0 r$ with respect to the propagation direction. When used to illuminate a spinning object, this incline results in a frequency shift of the scattered light similar to that obtained in Doppler velocimetry.

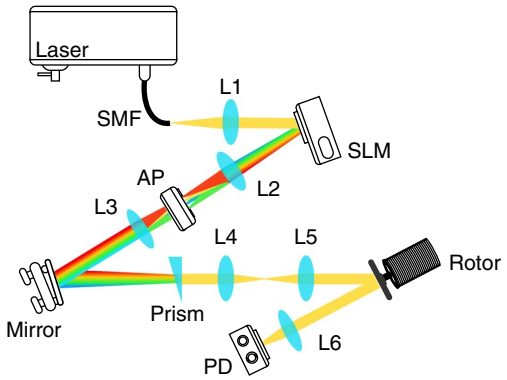

Fig. 2. A supercontinuum laser source is coupled into a single-mode fiber (SMF) to produce a spatially coherent beam of white light, which is then collimated by a lens, L1, and illuminates a spatial light modulator (SLM). The SLM is encoded with a combination of fork diffraction patterns, such that the first-order diffracted beam is of the desired OAM superposition ℓ. A spatial filter, AP, is placed in the focal plane of a lens, L2, and used to select the first-order diffracted beam of all the wavelength components. To compensate for chromatic dispersion resulting from the diffraction grating, the first-order beam is then reimaged onto a prism, yielding a white-light OAM-carrying beam within which all the wavelength components are coaxial. This white OAM is reimaged onto the spinning rough surface, and the backscattered light is collected by a photodetector, PD, to measure the intensity modulation frequency.

The linear Doppler shift is usually associated with the line-of-sight component of velocity between the source and observer. However, the Doppler effect can also be observed from transverse motion. If a moving rough surface is illuminated at an oblique angle, the light of frequency ω_0 scattered at normal incidence is subject to a reduced Doppler shift given by $\Delta\omega = (\omega_0 \sin \alpha)v/c$, where α is the angle between the illumination and the surface normal and v is the transverse velocity of the surface. Oblique illumination can take many forms; light is normally represented as a plane wave, but other phase structures are also possible. In particular, light beams with helical phasefronts, i.e., with a phase structure described by $\Psi(\phi) = \exp(i\ell\phi)$, carry an OAM of $\ell\hbar$ per photon [12,13]. These helical phasefronts correspond to a local skew angle of the Poynting vector (or local ray direction) of $\beta = \ell/k_0 r$, where k_0 is the wave number and r is the radius vector [14] (see Fig. 1). Consequently, for a surface spinning with an angular velocity Ω, and illuminated by a light beam with helical phasefronts, the on-axis scattered light is subject to a frequency shift of $\Delta\omega = \Omega\ell$. We note that, unlike the linear Doppler shift, this angular Doppler shift is independent of the frequency of the incident light and hence should be observable as a single shift for a scattered white-light beam. Rather than measure this frequency shift directly, it is convenient to create an illumination beam comprising two different values of OAM, ℓ_1 & ℓ_2, such that the scattered light comprises two different frequency components that interfere to produce a modulation in the detected intensity, $f_{\text{mod}} = \Omega|\ell_1 - \ell_2|/2\pi$.

Figure 2 shows the experimental arrangement for observation of the white-light rotational Doppler shift. A supercontinuum white-light source (Fianium SC400-6) is coupled to a single-mode fiber to define the light's spatial coherence. The output from this fiber is allowed to diverge and then collimated to illuminate a spatial light modulator (SLM). If the SLM is programmed with a simple diffraction grating containing an on-axis fork singularity, the resulting first-order diffracted beam possesses helical phasefronts [15]. The approach can readily be extended to create superpositions of helically phased beams [16], in our case with indices ℓ_1 and ℓ_2. The combination of a diffractive approach and a broad spectral source means that this first-order light is subject to angular dispersion. This angular dispersion is compensated by an appropriate prism placed in the image plane of the SLM, resulting in a collimated white-light beam with the chosen modal structure [17]. This phase-structured white-light beam is reimaged to the rotation axis of the scattering surface. The details of the scattering surface are not critical to the observation of the rotational Doppler effect. In this case the surface was plastic, of rough texture on the scale of a millimeter, and sprayed with a silver paint. The scattered light is then collected by a large-aperture lens and relayed to a large-area photodiode. Note that in this configuration the modal selectivity comes from the illumination light and the detection system is multimodal. However, as demonstrated in our earlier work, the modal selectivity can instead be incorporated into the detection system [9]. The output of this photodiode is acquired by computer, digitized, and Fourier transformed such that the frequencies of the resulting intensity fluctuations can be observed and recorded. The rotational speed of the surface could also be recorded and logged using a simple optical pulse counter measuring the periodic signal from a reflective mark on the rotation axle.

Figure 3 shows a typical power spectrum of the intensity fluctuations recorded in the white light that is backscattered from the spinning surface. Figure 4 is a graph showing the

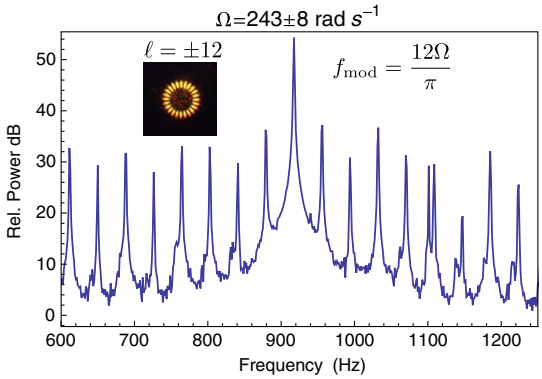

Fig. 3. The recorded time sequence of the intensity backscattered from the spinning surface is Fourier transformed to give a power spectrum from which the peak modulation frequency in this backscattered light can be measured. The power normalization is with respect to the noise floor of the detector (0 dB). The inset shows the intensity cross section of the OAM superposition $\ell = \pm 12$.

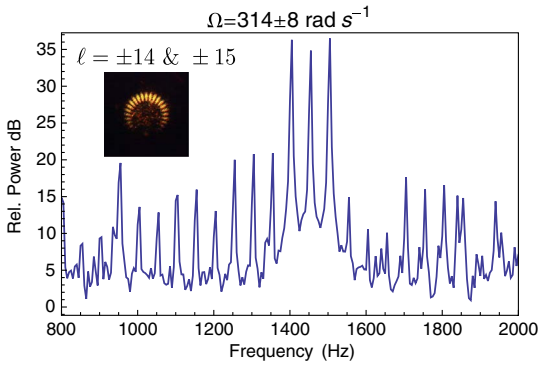

Fig. 5. The observed power spectrum in the intensity modulation of the scattered light obtained spinning surface is illuminated with a superposition of $\ell = \pm 14$ & ± 15. This superposition results in a cluster of peaks, corresponding to the integer differences between the various OAM components of the illuminating light. The power normalization is with respect to the noise floor of the detector (0 dB). The inset shows the intensity cross section of the OAM superposition $\ell = \pm 14$ & ± 15.

measured frequency of the largest peak in the power spectrum as a function of both the spin rate of the surface and the modal superposition of the illumination (insets show the intensity structure of the illumination beam). In each case, the intensity cross section of the illuminating beams corresponds to a petal pattern with $|\ell_1 - \ell_2|$ rotational symmetry. As anticipated, the power spectrum reveals a peak in the intensity modulation at an angular frequency $f_{\mathrm{mod}} = \Omega|\ell_1 - \ell_2|/2\pi$. This peak is approximately 20 dB above various other peaks at frequencies corresponding to integer differences $|\ell_1 - \ell_2|$. The origin of these additional peaks is consistent with modal impurities that are inherent in either lateral or angular misalignment of the illumination beam and/or slight aberrations in the optical system [18]. The main source of uncertainty in our results is not the identification of the peak in the power spectrum; rather, it is the uncertainty in the stability and measurement of the rotation speed of the motor to which the scattering surface is attached. This uncertainty in rotation speed is $\approx \pm 1$ Hz, equivalent to $\approx \pm 7$ rads^{-1}.

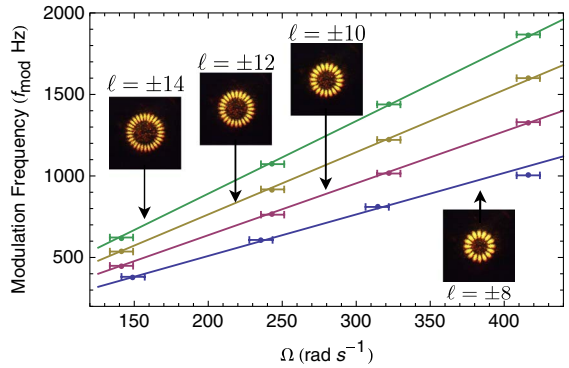

Fig. 4. Observed modulation frequency plotted as a function of rotation rate for four different superpositions of illuminating OAM, $\ell = \pm 8, \pm 10, \pm 12, \pm 14$. The predicted frequency of the intensity modulation is $f_{\mathrm{mod}} = \Omega|\ell_1 - \ell_2|/2\pi$, shown as a solid line. The insets show the intensity cross section of the various OAM superpositions.

To explore the influence of modal composition on the measured power spectrum, we deliberately created an illumination beam comprising multiple OAM modes. Figure 5 shows a specific example of the power spectrum obtained when the illuminating beam is an OAM superposition of $\ell_1 = 14$ & 15 and $\ell_2 = -14$ & -15. As anticipated, we observe significant peaks at modulation frequencies corresponding to 28 and 30 Ω, but we also observe a peak at 29 Ω. This latter peak corresponds to the interference between $\ell = \pm 14$ and $\ell = \mp 15$. The presence of this latter peak emphasizes that for modal superpositions, rather than obtaining a single-valued frequency shift that scales with the average OAM values, the spectrum comprises individual peaks that correspond to the pure OAM modes contained within the modal superposition. It is this last result that demonstrates that the OAM is the natural basis in which to both describe and calculate this rotational Doppler effect.

In this work we have observed the rotational Doppler shift within white light backscattered from a rotating object. We have shown that unlike the linear Doppler effect, the rotational Doppler effect is achromatic, in that all spectral components are shifted by the same frequency. We have also shown that OAM is the natural choice of basis set where, within a modal superposition, it is the individual pure OAM modes that give rise to an independently observable frequency shift. The observability of the rotational Doppler shift even for white-light sources suggests its applicability for the remote sensing of rotating objects. Applications for remote sensing based on this rotational Doppler shift have been suggested in various astronomical situations [19] but should also be applicable to terrestrial applications.

FUNDING INFORMATION

Engineering and Physical Sciences Research Council (EPSRC)—COAM (EP/I012451/1); European Research Council (ERC)—TWISTS; The Royal Society.

REFERENCES

1. T. Asakura and N. Takai, Appl. Phys. **25**, 179 (1981).
2. R. Meynart, Appl. Opt. **22**, 535 (1983).
3. B. A. Garetz, J. Opt. Soc. Am. **71**, 609 (1981).
4. I. Bialynicki-Birula and Z. Bialynicka-Birula, Phys. Rev. Lett. **78**, 2539 (1997).
5. J. Courtial, K. Dholakia, D. A. Robertson, K. Dholakia, L. Allen, and M. J. Padgett, Phys. Rev. Lett. **80**, 3217 (1998).
6. S. Barreiro, J. W. R. Tabosa, H. Failache, and A. Lezama, Phys. Rev. Lett. **97**, 113601 (2006).
7. A. Belmonte and J. P. Torres, Opt. Lett. **36**, 4437 (2011).
8. F. C. Speirits, M. P. J. Lavery, M. J. Padgett, and S. M. Barnett, Opt. Lett. **39**, 2944 (2014).
9. M. P. J. Lavery, F. C. Sperits, S. M. Barnett, and M. J. Padgett, Science **341**, 537 (2013).
10. C. Rosales-Guzmån, N. Hermosa, A. Belmonte, and J. P. Torres, Sci. Rep. **3**, 2851 (2013).
11. L. Allen, M. Babiker, and W. L. Power, Opt. Commun. **112**, 141 (1994).
12. L. Allen, M. W. Beijersbergen, R. J. C. Spreeuw, and J. P. Woerdman, Phys. Rev. A **45**, 8185 (1992).
13. A. M. Yao and M. J. Padgett, Adv. Opt. Photon. **3**, 161 (2011).
14. J. Leach, S. Keen, M. J. Padgett, C. Saunter, and G. D. Love, Opt. Express **14**, 11919 (2006).
15. V. Y. Bazhenov, M. V. Vasnetsov, and M. S. Soskin, JETP Lett. **52**, 429 (1990).
16. S. Franke-Arnold, J. Leach, M. J. Padgett, V. E. Lembessis, D. Ellinas, A. J. Wright, J. M. Girkin, P. Öhberg, and A. S. Arnold, Opt. Express **15**, 8619 (2007).
17. A. J. Wright, J. M. Girkin, G. M. Gibson, J. Leach, and M. J. Padgett, Opt. Express **16**, 9495 (2008).
18. M. V. Vasnetsov, V. A. Pas'ko, and M. S. Soskin, New J. Phys. **7**, 46 (2005).
19. M. Harwit, Astrophys. J. **597**, 1266 (2003).